PHYSICAL REVIEW B VOLUME 22, NUMBER 10 15 NOVEMBER 1980

Inelastic Mie scattering from rough metal surfaces: Theory and experiment

J. I. Gersten
Department of Physics, The City College of the City University of New York, New York, New York 10031

D. A. Weitz, T. J. Gramila, and A. Z. Genack
Exxon Research and Engineering Company, P.O. Box 45, Linden, New Jersey 07036

(Received 16 June 1980)

A theory for inelastic Mie scattering from rough metal surfaces or metal sols is proposed. A resonant excitation of a localized dipolar plasmon can enhance the cross section, and experimental data relating to the phenomenon in silver and copper are presented. Two distinct effects are noted. One is inelastic light scattering from the rough metal surface or bare metal sol. The other is related to Reyleigh scattering from adsorbed molecules as modified by the presence of the substrate. Both involve frequency shifts determined by the characteristic mechanical vibrations of the metal. A striking feature of this inelastic Mie scattering is that for a distribution of particle sizes and shapes the frequency shift changes as the incident laser frequency is changed or as the index of refraction of the surrounding medium is changed. Inelastic Mie scattering is shown to yield important information on the surface roughness required for the observation of surface-enhanced Raman scattering.

I. INTRODUCTION

Raman scattering (RS) is one of the most versatile tools available in the field of molecular physics. For large molecules, however, the number of Raman components often grows to the point where interpretation of the spectra becomes difficult. In principle, Raman scattering exists for objects of any size and, in fact, is of great value in macroscopic solid-state physics where translational symmetry leads again to simple spectra. In this paper we focus our attention on a range of particle sizes intermediate between molecular and macroscopic, i.e., 10–1000 Å. Particles of such sizes are often studied using Mie scattering,[1] which is basically elastic light scattering. In this paper we examine inelastic Mie scattering which is caused by scattering from mechanical oscillations of the particle itself. The frequency shifts involved are small compared with typical optic-mode frequencies but are higher than typically seen in Brillouin scattering. By studying vibrations which modulate the size and shape of the particle we are able to get information about the distribution of particle sizes.

To overcome the normally weak intensity of inelastic light scattering, we consider the case where the excitation energy is tuned to an electronic resonance of the small particle, leading to the possibility of large enhancements in the RS cross section. In this paper, we consider only metallic particles and consider only the lowest-order resonance, the dipolar plasmon. However, higher-order electronic resonances will exist, in principle, for both metallic and dielectric particles. We approximate the case of metal sols by taking the particles to be spheroids. When studying rough metal surfaces, we model the surface as hemispheroids protruding from a plane. In the simplest cases we will be interested in the bare particle or rough surface itself immersed in a dielectric medium. However, we shall also be concerned with the effect produced by the presence of adsorbed molecules.[2] The basis of these studies is the model which was recently utilized in the explanation of the phenomenon of surface-enhanced Raman scattering (SERS)[3,4] from rough surfaces with adsorbed molecules. We focus our attention here primarily of spheroids, so the theory applies directly to the case of metal sols. However, only minor modifications to the theory are necessary for its application to metal surfaces.

The theory reported in this paper was developed to account for the observation on an extremely intense, very-low-frequency mode observed in RS from roughened metal electrode surfaces of the type which exhibit SERS.[4] The low-frequency RS has rather unusual behavior, which we explain using this theory of inelastic Mie scattering. This paper includes a summary of the experimental results and a comparison with the theory.

In Sec. II the theory for inelastic Mie scattering from small metal particles is presented. The relationship of these concepts to the origin of SERS is discussed and the scale of roughness and the range of excitation frequency required for the observation of SERS are set forth. In Sec. III we present experimental results for low-frequency RS from roughened silver and copper electrode surfaces as well as from silver sols. The results of experiments with and without adsorbed organic molecules are discussed. In Sec. IV we consider and reject various alternate explanations of the observed low-frequency mode. We treat in detail

the possibility that the mode is due to Brillouin scattering from a composite material consisting of silver spheres in a dielectric matrix with a large increase in the index of refraction due to a collective resonance of the colloidal spheres. Finally we summarize our results and conclude in Sec. V.

II. THEORY

Consider a spheroid of semimajor axis a, semiminor axis b, and dielectric constant $\epsilon(\omega)$ in a solution of optical dielectric constant ϵ_s. We shall be concerned with the case where the size of the spheroid is small compared with the excitation wavelength, i.e., $\omega a \epsilon_s^{1/2}/c \ll 1$, so that retardation effects can be neglected. We also limit our attention to spheroids separated by more than $\lambda \epsilon_s^{-1/2}$ so that cooperative effects involving neighboring spheroids[5] may be neglected. For the sake of simplicity we assume that the incident radiation electric field $\vec{E}_0$ is directed along the major axis. This description is sufficient for studying the light scattering produced by the bare particle. As we shall also be concerned with the effects of an adsorbed molecule, let us position a molecule of polarizability α a distance H from the apex along the major axis. (More generally α denotes the appropriate diagonal matrix element of the polarizability tensor.) We further simplify matters by neglecting the role of magnetic dipole scattering, which was already found to be small.[3]

In order to compute the light scattering we start with an expression for the total electric dipole moment of the molecule-spheroid system[3]:

$$D = \frac{f^3 E_0 \xi_0 [\epsilon(\omega) - \epsilon_s]}{3\Delta} + \frac{\alpha E_0}{1-\Gamma}\left(1 + \frac{\xi_0 Q_1'(\xi_1)[\epsilon_s - \epsilon(\omega)]}{\Delta}\right)^2, \quad (1)$$

where $Q_n(\xi_1)$ is a Legendre function of the second kind, $f = (a^2 - b^2)^{1/2}$, $\xi_0 = a/f$, $\xi_1 = \xi_0 + H/f$, and $\Delta = \epsilon(\omega) Q_1(\xi_0) - \xi_0 \epsilon_s Q_1'(\xi_0)$. An expression for Γ has been derived and found to be numerically small for most cases of interest,[3] so it will be neglected here. In Eq. (1) the first term is the dipole moment that would be induced on the spheroid in the absence of an adsorbed molecule, while the second term is the modification produced by the presence of the molecule.

The condition $\mathrm{Re}\Delta = 0$ defines the dipolar plasmon for the spheroid and marks the frequency at which a strong dipole moment develops in response to an applied field. It is this resonant increase in the total dipole that may lead to an increase in the inelastic scattering intensity from the spheroid. We note also that the role of plasmons in the phenomenon of SERS has been recognized by a number of authors on both experimental[4,6] and theoretical grounds.[3,7] A graph of this plasmon frequency as a function of aspect ratio a/b for several indices of refraction ($n = \epsilon_s^{1/2}$) is given in Fig. 1 for Ag, Au, and Cu. The function $\epsilon(\omega)$ used in determining these curves is that reported in the literature and

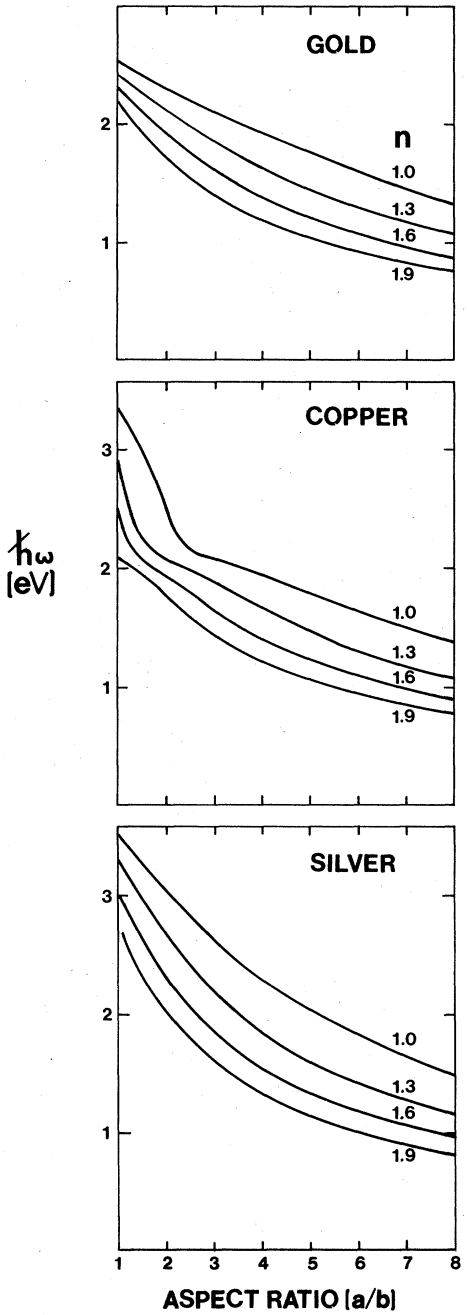

FIG. 1. Plasmon energy as a function of aspect ratio of the spheroid for different metals and different indices of refraction of the surrounding medium n. The plasmon energy is defined by the solution of $\mathrm{Re}(\Delta) = 0$.

was obtained from experiments on bulk samples.[8]

When the resonance condition is met, $\mathrm{Re}\Delta=0$, the amplitude of the dipole will be limited by $\mathrm{Im}\epsilon(\omega)$ for ϵ_s real. The damping of the dipolar plasmon caused by an increase in $\mathrm{Im}\epsilon(\omega)$ limits the enhancement in the RS and influences the range of excitation frequencies over which SERS can be observed. For example, the sharp increase in $\mathrm{Im}\epsilon(\omega)$ due to interband transitions above 2.0 eV for both Cu and Au (Ref. 8) is the source of the decrease in intensity of SERS observed on these metals as the excitation energy is increased above this value. In contrast, $\mathrm{Im}\epsilon(\omega)$ of Ag remains small to ~4.0 eV, and SERS on silver persists to much higher excitation energies. It should be noted, however, that once $\mathrm{Re}(\epsilon)$ becomes positive, the possibility for resonant enhancement due to the dipolar plasmon excitation is lost. This occurs at 3.8 eV for Ag, when $\epsilon_s=1$.

When considering particles of small size, care must be exercised in the choice of $\epsilon(\omega)$. Collisions with the particle's boundary relax the electronic motion and increase $\mathrm{Im}\epsilon(\omega)$ from the bulk value.[9] This is particularly severe when the major axis $2a$ is less than the bulk mean free path of the electron λ_e. The amplitude of the dipolar resonance is then reduced, as may be seen from Eq. (1). For Ag (where $\lambda_e \approx 430$ Å) this implies that particles with $a \leq 215$ Å will develop smaller dipoles and hence will be less efficient scatterers. Analogous ranges for Au and Cu are $a \leq 65$ Å and $a \leq 55$ Å, respectively.

In the second term in Eq. (1) the argument enclosed in large parentheses may be interpreted as an enhancement factor for the local field at the molecule's position. The development of a large local field hinges on the constructive interference of the fields produced by sources on different parts of the spheroid. For large particle sizes, retardation effects lead to destructive interference and the dipole is reduced in magnitude. Using the condition $\omega a \epsilon_s^{1/2} \gtrsim 1$ as the definition of the retardation domain we find that, for an excitation wavelength of 5000 Å, $a \geq 600$ Å will result in a decrease in the RS intensity due to retardation effects.

We note that the theory presented above has allowed us to determine two fundamental characteristics—the size and the shape—of the metal sols or of the surface roughness required to obtain the large enhancement in the RS. The optimum size of the roughness features is ~500 Å. large enough so that $\mathrm{Im}\epsilon(\omega)$ is not increased due to a size limitation of the electron mean free path, and small enough so that retardation effects do not limit the total dipole. The optimum shape is determined by the ellipticity required to achieve the dipolar resonance for a particular excitation energy. Thus we have a theoretical basis for a description of two key parameters characterizing the surface roughness required for SERS.

If one were to insert Eq. (1) into Larmor's formula and normalize to unit light intensity, one would obtain an expression for the ordinary Mie and Rayleigh scattering cross sections.[3] By allowing the shape of the spheroid to oscillate periodically in time we may obtain a formula for the cross section for inelastic Mie scattering. We will treat the solid as a perfectly elastic isotropic medium. In general a spheroid may have many modes of oscillation. The simplest is the breathing mode in which the size changes periodically but the shape remains essentially fixed. However, we expect the amplitude of this vibration to be small because of the difficulty in compressing the metal spheroid. Furthermore, since the plasmon frequency is determined by the shape (see Fig. 1) we do not expect this oscillation to produce significant modulation of the dipole. The next simplest mode is a spheroidal vibration in which the semimajor axis a varies harmonically in time and b lags behind by 180°. Higher-frequency modes involving angular structure around the spheriod or modes with nodes inside the spheroid do not lead to significant modulation of the aspect ratio of the spheroid and will be neglected.

For the spheroidal vibration of interest we take a to be of the form $a=a_0+A\cos\Omega t$ where A is the amplitude and Ω the angular frequency of the vibration. This mode will be slightly damped due to coupling to phonons of the liquid but this damping will be neglected here. (It may contribute, however, to the wings of the spectral lines.) The magnitude of A may be estimated by setting the elastic energy equal to one quantum of vibrational energy. Thus $M(\Omega A)^2 \sim \hbar\Omega$, where M is the mass of the spheroid. Introducing the density ρ yields the relation $A^2=\hbar/[\Omega f^3 \rho \xi_0(\xi_0^2-1)]$. To a good approximation we may write $b=b_0-B\cos\Omega t$, where $B \approx -\nu A$, ν being the Poisson ratio ($\nu_{\mathrm{Ag}}=0.38$, $\nu_{\mathrm{Cu}}=0.33$, $\nu_{\mathrm{Au}}=0.42$). As a and b oscillate, so will the volume of the spheroid and the number density of electrons within it. Thus one would expect oscillations in $\epsilon(\omega)$ as well.

In the neighborhood of the plasmon resonance, the inelastic Mie scattering cross section is obtained by differentiating Eq. (1) with respect to a. The dominant variation arises from the denominator Δ, so we make the approximation that only its derivative is retained. Thus

$$\frac{d\sigma}{d\omega'} \approx \frac{\pi A^2}{6}\left(\frac{\omega}{c}\right)^4 \left| \frac{f^3 \xi_0(\epsilon-\epsilon_s)}{3\Delta^2} + \frac{2\alpha(\epsilon-\epsilon_s)^2 \xi_0^2 [Q_1'(\xi_1)]^2}{\Delta^3} \right|^2 \times \left| \frac{\partial\Delta}{\partial a} \right|^2 \beta\hbar\Omega \left(\frac{\delta(\omega'-\omega-\Omega)}{\exp(\beta\hbar\Omega)-1} + \frac{\delta(\omega'-\omega+\Omega)}{1-\exp(-\beta\hbar\Omega)} \right), \tag{2}$$

where $\beta = 1/k_B T$, T being the temperature and k_B being Boltzmann's constant. In Eq. (2) we have included the appropriate Bose factors for the Stokes and anti-Stokes sidebands. Evaluation of $\partial\Delta/\partial a$ yields

$$\frac{\partial \Delta}{\partial a} = -f^{-1}[\xi_0 \nu(\xi_0^2 - 1)^{1/2} + \xi_0^2 - 1] \times [\epsilon Q_1'(\xi_0) - \epsilon_s \xi_0 Q_1''(\xi_0) - \epsilon_s Q_1'(\xi_0)] + Q_1(\xi_0)\frac{\partial \epsilon}{\partial a}. \tag{3}$$

A crude evaluation of $\partial\epsilon/\partial a$ based on the Drude expression $\epsilon = 1 - \omega_p^2/\omega(\omega + i/\tau)$ [where $\omega_p^2 = 4\pi N e^2/mV$, N being the number of conduction electrons and V the volume of the spheroid ($V = 4\pi a b^2/3$)] yields

$$\frac{\partial \epsilon}{\partial a} = (1 - \epsilon) f^{-1}[\xi_0^{-1} - 2\nu(\xi_0^2 - 1)^{-1/2}].$$

It is, perhaps, instructive to interpret Eqs. (1) and (2) from a quantum-mechanical point of view. For illustrative purposes let us do this via Feynman diagrams. The basic ingredients are photons (to be denoted by curvy lines), electrons (solid lines), plasmons (dashed lines), and phonons (dotted lines). Since we are concerned with a particle of finite extent, the plasmon and photon may couple directly. The electron of concern is located on the molecule. The electrons of the spheroid are treated collectively.

In Fig. 2(a) the various contributions to the matrix element of Eq. (1) are depicted. The square box symbolizes the entire matrix element. The first diagram represents the dipolar scattering from the plasmon resonance of the metal spheroid. The remaining four diagrams correspond to the second term of Eq. (1). The circle denotes excitation of the molecule from the ground state (a) to some excited state (n), with or without plasmon excitation. It is decomposed explicitly in Fig. 2(b), and a summation of such terms accounts for the denominator $1 - \Gamma$.

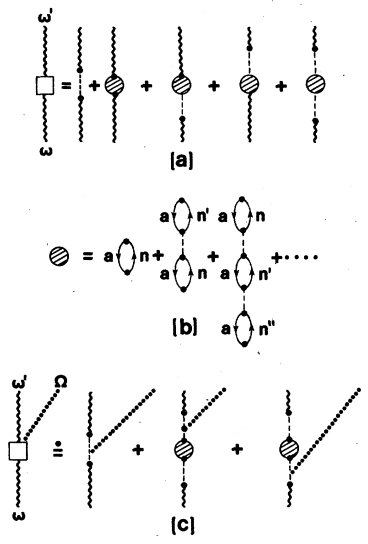

FIG. 2. Feynman diagrams for the light scattering processes of Eqs. (1) and (2); (a) representation of dipolar scattering from the plasmon; (b) scattering from the molecule leading to $1 - \Gamma$ denominator, and (c) scattering including a phonon leading to Eq. (2) and showing the origin of the $1/\Delta^3$ denominator.

In the analogous way we may place a phonon insertion in the diagrams of Fig. 1 and obtain the Raman amplitudes. The terms appearing in Eq. (2) (which is approximate) are illustrated in Fig. 2(c). The Δ^{-3} behavior is accounted for in terms of the three plasmon propagators.

An improvement of the classical formula equation (2) may be obtained by studying Fig. 2(c). In Eq. (2) the plasmon propagator is given by $1/\Delta(\omega)$, where ω is the incident photon energy. However, after a phonon is emitted (with frequency Ω) the remaining plasmon energy is reduced to $\omega - \Omega$. Therefore the new propagator should be $1/\Delta(\omega - \Omega)$. Thus the first term in Eq. (2) should have $1/[\Delta(\omega)\Delta(\omega - \Omega)]$ in place of $1/[\Delta(\omega)]^2$. Likewise by examining the two remaining diagrams of Fig. 3 we conclude that in place of $2/[\Delta(\omega)]^3$ a more appropriate expression is

$$1/[\Delta^2(\omega)\Delta(\omega - \Omega)] + 1/[\Delta(\omega)\Delta^2(\omega - \Omega)].$$

Since Ω is small compared with the width of $|1/\Delta(\omega)|$, however, we expect this to be a minor correction. For molecular modes in SERS, however, the replacement of $1/[\Delta(\omega)]^2$ by $1/[\Delta(\omega)\Delta(\omega - \Omega)]$ has a more important effect, since Ω for a molecular vibration frequency can be of the same order of magnitude as the width of $|1/\Delta(\omega)|$. (Such quantum effects will be discussed in more detail elsewhere.)

On naive dimensional grounds we expect an acoustic vibration frequency on the order of $\Omega = \pi v/a$, where v is the speed of a dilatational wave. (Shear waves are not expected to produce a variation of the shape of the spheroid and thus not be effective in producing side bands.) More confidence in this expression is gained by considering a symmetric vibration of the spheroid in detail. A wave emanating from one focal point. The disrection strikes the bounding surface and is reflected towards the other focal point. The distance traveled is $2f\xi_0$. If this wave is to arrive in phase with the oscillation at the second focal point, one full period must have elapsed. This again leads to $\Omega = \pi v/a$. The above argument, unfortunately, is not rigorous due to the complicated nature of the boundary conditions. When re-

peated for a sphere, where an analytic solution does exist,[10] one finds

$$\Omega = \pi\kappa v/a\,, \tag{4}$$

where $\kappa = 0.84$. Thus we expect κ for a spheroid to depart from unity by on the order of 15%. We expect the hemispheroid protrusion on a rough metal surface to have a similar spheroidal mode with approximately the same frequency.

We model the sol and rough metal surface as consisting of, respectively, spheroidal and hemispheroidal particles with a distribution of a and b values governed by some distribution function $P(a,b)$. According to Eq. (4) we expect a direct correlation between values of a and Ω. The resonance condition, $\mathrm{Re}\Delta = 0$ defines the position of the peak contribution to the inelastic Mie scattering in the distribution of spheroids. The resonance condition is very sharp (with a width determined by $\epsilon_2(\omega)$, which is small for the ω of interest and effectively allows us to relate a given value of ω to a given aspect ratio a/b. Thus a measurement of the line shape for inelastic Mie scattering may aid in the measurement of the distribution function $P(a,b)$.

III. EXPERIMENT

We expect from Eq. (4) that the frequency of the inelastic Mie scattering will be several wave numbers for $v = 3\times10^3$ m/sec and a typical 250-Å particle. We have, in fact, observed an intense peak in the low-frequency RS from rough metal surfaces.[4] A rough silver or copper surface was prepared by a mild annodization[11] of an electrode in a cell containing an electrolyte of 0.1M KI in water. A backscattering optical geometry was used to observe RS from the surface, and the scattered radiation was dispersed with a Spex (1401) double monochromator equipped with a third monochromator scanned in tandem. All the gratings were holographic and the slits were set to a bandpass of ~0.2 cm^{-1} to give sufficient rejection of the elastically scattered radiation to observe RS within ~2.0 cm^{-1} from the laser line. For an Ag electrode, excited with the 5145-Å Ar^+ laser line, we observe an intense peak at a frequency, $\Omega \approx 9$ cm^{-1}, as shown in Fig. 3. The peak is RS from the metal itself[4] as the complete spectrum contains no molecular modes of surface-adsorbed organic molecules. The addition of a surface-adsorbed organic molecule causes an increase in the intensity of the low-frequency RS, but no change in Ω.

When ω_{ex} is varied we observe a dramatic shift in Ω, as shown in Fig. 4. These data were taken using an electrolyte containing 0.1 M KBr and

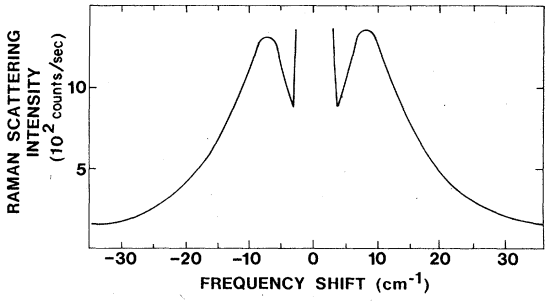

FIG. 3. Low-frequency RS from a silver electrode surface prepared in 0.1M KI in water. Both the anti-Stokes (negative frequency shift) and Stokes scattering are shown. Excitation is with $\lambda_{ex} = 514.5$ nm.

0.05M pyridine. The theory can be used to model this behavior if we assume that the distribution of a and b values are independent, so $P(a,b)$ factors, i.e., $P(a,b) = P_1(a)P_2(b)$, where $P_2(b)$ is sharply peaked at some value b_p. For a given value of ω we select a given parameter ξ_p as the root to the equation $\mathrm{Re}\Delta = 0$, or

$$\frac{\xi_p Q_1'(\xi_p)}{Q_1(\xi_p)} = \frac{\mathrm{Re}\epsilon(\omega)}{\mathrm{Re}\epsilon_s}\,. \tag{5}$$

The corresponding peak in the inelastic Mie scattering occurs at

$$\Omega_p = \frac{\pi v(\xi_p^2 - 1)^{1/2}}{b_p \xi_p}\,. \tag{6}$$

Equations (5) and (6) define a relation between the excitation frequency and the peak of the inelastic Mie scattering for the assumed $P_2(b)$. As the

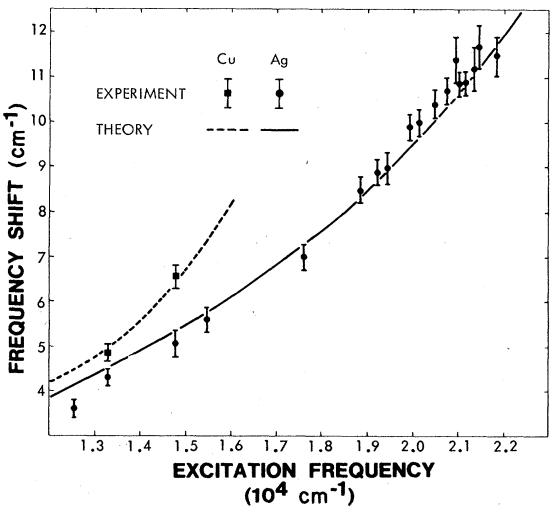

FIG. 4. Variation in frequency shift Ω of the inelastic Mie scattering with excitation frequency for silver and copper electrodes prepared in electrolytes containing 0.1M KBr and 0.05M pyridine in water. The predictions of the theory are also shown.

laser frequency is varied, it resonates with specific spheroids. These spheroids, in turn, have characteristic "acoustic" frequencies that appear as the inelastic Mie sidebands. This leads to the remarkable fact that the Raman shift is changed in a continuous manner as the primary laser frequency is changed. We obtain the good agreement with data shown in Fig. 4 using $v = 3.0 \times 10^3$ m/sec and $b_p \sim 50$ Å for silver. Agreement is also obtained for copper using $v = 4.8 \times 10^3$ m/sec and $b_p \sim 40$ Å, although, like SERS, the data on the low-frequency mode is limited to excitation in the red. The large difference in slope between the data of copper and silver is accurately predicted by the theory and is due to the different behavior of $\mathrm{Re}\epsilon(\omega)$, causing the difference in the behavior of the plasmon frequencies shown in Fig. 1.

We also observe a shift in Ω when ω_{ex} is kept constant and the index of refraction of the surrounding dielectric medium n is varied. This was accomplished by preparing a rough surface under normal conditions in an electrolyte of water and 0.1M KI. After obtaining the low-frequency RS spectrum, the electrolyte was replaced by nitrogen gas and the surface allowed to dry. A second RS spectrum was obtained and the results are shown in Fig. 5. We see that Ω decreases as n is decreased, in accord with the behavior of the plasmon resonant frequency as predicted by the theory, using Eq. (5) and illustrated in Fig. 1. We note that the removal of the liquid and the drying of the electrode may change the structure of the surface somewhat. However, in all cases tried, we observed a decrease in Ω when n was decreased in qualitative agreement with the theory. We observed a similar decrease in Ω for rough, evaporated, thin-film silver surfaces exposed to air.

The anomalous shift in Ω with ω_{ex}, in a case where the Raman shift does not depend on the scattering wave vector, is, to our knowledge, unique to inelastic Mie scattering. It is, however, somewhat reminiscent of resonant RS where the relative amplitude of scattering from different

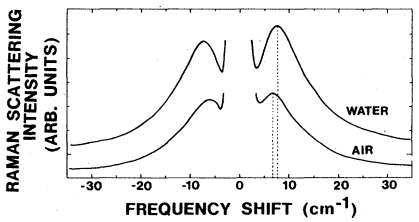

FIG. 5. Low-frequency RS from a silver electrode surface prepared in 0.1M KI in water taken with two different surrounding dielectric media: water ($n = 1.33$) and air ($n = 1.0$). Note the change in Ω. Excitation is with $\lambda_{ex} = 514.5$ nm.

modes can change due to variations in the electronic-vibrational coupling as the primary laser frequency is changed. In the case of inelastic Mie scattering from a distribution of particles, the vibrational modes can be regarded as a continuum, and the relative strength of the electron-phonon coupling for different parts of the continuum changes as different electronic states are resonantly selected. This results in the variation of the frequency of the peak scattered intensity as the excitation energy is varied.

On the basis of Eq. (2) we may expect the adsorption of molecules to considerably increase the cross section for inelastic Mie scattering. The bare Mie scattering contribution goes as $f^6 |\Delta|^{-4}$, whereas the presence of the molecule introduces a term varying as $\alpha^2 |\Delta|^{-6}$. For narrow enough plasmon resonances the latter term may be expected to dominate.

The effects of the inelastic Mie scattering due to the molecule can be observed experimentally. Figure 6 shows low-frequency RS spectra of a silver electrode prepared in an electrolyte containing 0.1M KBr in water, with increasing amounts of pyridine. The electrode was anodized the same way in each case. We can approximately calibrate the surface coverage by using the intensity of the pyridine mode at 1008 cm^{-1}. The intensity of the 1008-cm^{-1} line is not visible for concentration below 10^{-3} M and the line intensity increases with increasing pyridine concentration. As can be seen in Fig. 6, the intensity of the low-frequency mode increases as the pyridine surface coverage increases, in accord with Eq. (2). In fact, at the highest coverages, the molecular contribution appears to dominate that of the bare metal.

We have also observed enhanced inelastic Mie scattering from a sol. We study a system with contributions from both the bare metal and the adsorbed molecule. It was recently shown that the addition of small amounts of pyridine to silver

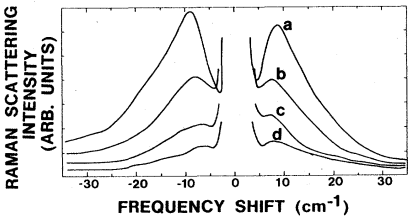

FIG. 6. Low-frequency RS from a silver electrode surface prepared in 0.1M KBr in water with a different solution concentration of pyridine: (a) $5 \times 10^{-2} M$, (b) $5 \times 10^{-3} M$, (c) $5 \times 10^{-4} M$, and (d) $5 \times 10^{-5} M$. Note the increase in intensity of the low-frequency mode with increasing pyridine concentration. No molecular pyridine lines are observable for concentrations below $\sim 10^{-3} M$. Excitation was with $\lambda_{ex} = 514.5$ nm.

sols, consisting of small spherical particles, caused an agglomeration of the particles which were then coated by pyridine.[12] This surface-adsorbed pyridine also showed surface-enhanced Raman scattering. We expect this system to consist of a distribution of spheroidal particles (or perhaps, more generally, ellipsoidal particles), which, as shown in Fig. 1, will lower the dipolar plasmon resonance to an energy accessible to a standard ion laser. Absorption measurements, in fact, show a shift in the absorption to lower energies.[12] Furthermore, the presence of the adsorbed molecules will give additional enhancement of the inelastic Mie scattering intensity. Such sols were prepared and excited with a focused beam of 514.5-nm Ar^+ laser radiation. The scattered radiation was collected at 90° and imaged on the slits of the monochromator. We show a low-frequency RS spectrum of both the Stokes and anti-Stokes side in Fig. 7. There is again an intense peak at a frequency shift, $\Omega \sim 8\ \mathrm{cm}^{-1}$, due to the inelastic Mie scattering from the metal sols themselves. Using Eq. (4) with $v = 3.0 \times 10^5$ cm/sec we estimate $b \sim 50$ Å for the size of particles contributing with an aspect ratio of ~3.

We also attempted to see the inelastic Mie scattering from the bare metal sols. Before the addition of the pyridine, the sol particles are smaller and are more nearly spherical, exhibiting an absorption band centered at ~380 nm (Ref. 12), in agreement with the prediction of Eq. (5) (see Fig. 1). We excited with frequencies near this absorption resonance, using the 4680- and 4131-Å lines of a Kr^+ laser. However, we were unable to see any low-frequency RS. We attribute this to an increase in the effective $\mathrm{Im}\epsilon(\omega)$ of the very small sol particles caused by the additional boundary scattering of the electrons, decreasing the strength of the resonance. Furthermore, the bare sols do not have a highly polarizable surface-adsorbed organic molecule which would increase the intensity of the low-frequency RS.

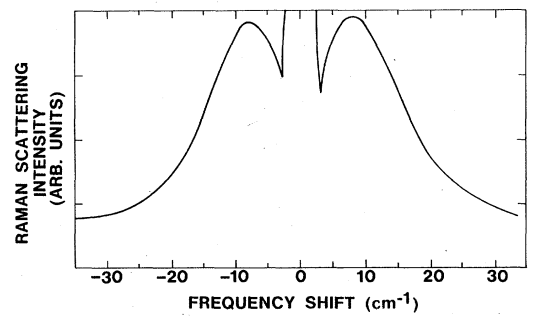

FIG. 7. Low-frequency RS from pyridine-coated silver sols excited with $\lambda_{ex} = 514.5$ nm.

IV. AN ALTERNATE HYPOTHESIS

It has been proposed that the excitation of a collective resonance in a colloid of metal spheres is intimately connected with the phenomenon of SERS.[13] Our goal in this section will be to see how the existence of the low-frequency mode can be fit into such a picture. One possibility is that it is due to Brillouin scattering with higher-frequency shifts than typically observed because of an increase in the index of refraction of the composite medium n_m. Let us compute the expected Brillouin frequency shift Ω.

Let the angle between the incident and scattered radiation in the medium be θ. Let v_m denote the effective speed of sound of the colloid and n_m denote the index of refraction of the colloid. The momentum transfer is

$$Q = \frac{2\omega n_m}{c} \sin\frac{\theta}{2}, \tag{7}$$

and the Brillouin shift is

$$\Omega = Q v_m. \tag{8}$$

We shall specify to the case of a backscattering geometry ($\theta = \pi$), and consider only spherical metal particles. Calculations for ellipsoidal metal particles show the same qualitative behavior as reported below for spheres.

Both n_m and v_m will depend on the volume fraction occupied by the metal spheres q. According to the Maxwell-Garnett theory[5] the effective dielectric constant is

$$\epsilon_m = \epsilon_s \frac{\epsilon + 2\epsilon_s + 2q(\epsilon - \epsilon_s)}{\epsilon + 2\epsilon_s - q(\epsilon - \epsilon_s)}, \tag{9}$$

where ϵ_s is the solvent dielectric constant and ϵ is the complex dielectric constant of the metal. In terms of ϵ_m, we have

$$n_m = [\tfrac{1}{2}(\mathrm{Re}\epsilon_m + |\epsilon_m|)]^{1/2}. \tag{10}$$

The condition for a collective resonance of the medium is

$$\mathrm{Re}\epsilon_m = 0, \tag{11}$$

in which case

$$n_m \to (\tfrac{1}{2}\mathrm{Im}\epsilon_m)^{1/2}. \tag{12}$$

Surface collective resonances where $\mathrm{Re}\epsilon_m = -\epsilon_s$ could be treated in a similar fashion.

One may obtain an expression for v_m in terms of the speed of sound in the metal v, the speed of sound in the solvent v_s, and their respective densities ρ and ρ_s. The speeds of sound may be written as $v_m = (B_m/\rho_m)^{1/2}$, $v = (B/\rho)^{1/2}$, and $v_s = (B_s/\rho_s)^{1/2}$, where B_m, B, and B_s are bulk moduli. An elementary argument concerning the compressibillty of the colloid leads to $B_m^{-1} = qB^{-1} + (1-q)B_s^{-1}$.

The composite density is $\rho_m = q\rho + (1-q)\rho_s$. Thus

$$v_m = \left[\left(\frac{q}{v}\right)^2 + \left(\frac{1-q}{v_s}\right)^2 + q(1-q)\left(\frac{\rho}{\rho_s v_s^2} + \frac{\rho_s}{\rho v^2}\right)\right]^{-1/2}. \tag{13}$$

For the case of sols consisting of silver balls in water the relevant parameters are $v = 3.0 \times 10^5$ cm/sec, $v_s = 1.5 \times 10^5$ cm/sec, $\rho = 10.5$ g/cm^3, and $\rho_s = 1.0$ g/cm^3. The dielectric constant of silver was taken from the literature and a value of $\epsilon_s = 1.69$ was employed. In Table I we list the various quantities of interest as a function of q. As the packing fraction q grows, the resonance energy $\hbar\omega$ drops, and the index of refraction at resonance is calculated to grow. Note that, on resonance, the imaginary and real parts of the index of refraction are equal, so the system becomes highly absorptive. The change in n_m with q will also cause a change in the Brillouin shift, Ω. This offers the possibility of a shift of Ω with ω_{ex}, if we assume an inhomogeneous distribution of volume packing fractions q, which allows a resonant matching over a wide range of excitation frequencies. The calculated Brillouin shift as a function of ω_{ex} is shown in Fig. 8. The Brillouin shift Ω is calculated to grow as the resonance energy drops. This is contrary to the experimental behavior of the low-frequency mode. The magnitude of Ω is also too small compared with the experiment, although the largest calculated values of Ω (for $\hbar\omega = 2.1$ eV) are caused by $q \sim 0.5$, where the simple Maxwell-Garnett theory used is no longer appropriate. The magnitude of Ω is further depressed if the finite mean free path of the electron is taken into account. Finally, it is interesting to note that the speed of sound in the medium is not a monotonic function of q, but in fact attains a mimimum at $q \sim 0.5$, due to the large density mismatch between the metal and the solvent.

Implicit in the above argument is that there exists an inhomogeneous distribution of volume packing fractions q, which allows a resonant matching over a wide range of frequencies. In the other extreme, however, we may regard q as having a unique value over the surface. Then excitation of the collective resonance occurs at a particular value of ω. At other excitation frequencies, n_m is not anomalously large and the predicted Ω would be of the same order of magnitude as measured in typical Brillouin experiments. These are typically $\lesssim 0.5$ cm^{-1} and are an order of magnitude lower than those we observe experimentally. We conclude that Brillouin scattering from the colloid could not adequately account for the experimental data. Thus the low-frequency RS is a purely molecular mode. In fact, our initial experimental data showing that the intensity of the low-frequency mode follows that of the molecular modes when the electrode voltage is varied, suggested that the mode might be due to a hindered rotation or libration of the surface-adsorbed molecule.[14] This type of mode would be expected to have a much lower frequency than any intramolecular mode. This interpretation was supported by a theory of Morawitz and Koehler,[15] who calculated the librational frequency of a molecule bound by its image in the metal, and obtained reasonable agreement with the experimentally observed frequencies. However, the subsequent observation of the mode on a bare metal surface, as well as the dependence of the frequency on ω_{ex} and n, and the lack of dependence of surface adsorbate argues in favor of an acoustic vibration of the metal. Furthermore, the present theory shows that inelastic Mie scattering intensity may be greatly increased by the presence of adsorbed molecules. This accounts for the fact that the intensity of the low-frequency mode follows that of the molecular modes over most of the range in which the molecule concentration or electrode voltage is varied. Perhaps RS from a low-frequency librational mode is obscured by the inelastic Mie scattering.

TABLE I. Quantities of interest for the Brillouin shift in the colloid. (It should be noted that for $q > 0.4$ the Maxwell-Garnett expression loses its validity. The values for $q > 0.4$ are included to illustrate the extrapolation.)

q	$\hbar\omega$ (eV)	n_m	Reϵ_m	Imϵ_m	Ω (cm^{-1})	v_m (cm/sec)
0.1	3.177	2.85	0	16.3	0.551	1.13×10^5
0.2	3.072	4.25	0	36.2	0.690	0.982×10^5
0.3	2.951	6.00	0	72.2	0.866	0.909×10^5
0.4	2.787	8.47	0	144	1.11	0.877×10^5
0.5	2.609	9.34	0	174	1.15	0.874×19^5
0.6	2.385	12.1	0	293	1.40	0.900×10^5
0.7	2.112	15.9	0	505	1.74	0.964×10^5
0.8	1.752	25.9	0	1350	2.67	1.09×10^5
0.9	1.259	45.0	0	4140	4.30	1.39×10^5

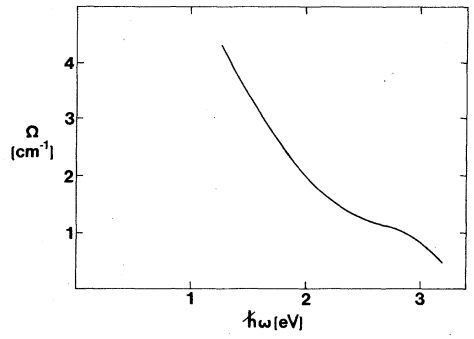

FIG. 8. Calculated Ω as a function of ω_{ex} for Brillouin scattering from a composite medium consisting of silver spheres in water. The concentration of spheres q is assumed to be inhomogeneous. The theory used is not valid for the regimes that produce the higher Ω($\lesssim$2.1 eV), and the results shown only illustrate the extrapolation (see Table I).

V. CONCLUSION

The theory presented in this paper agrees well with the experimental observations. However, the model treated is really most appropriate for the case of the metal sols. The very rough metal surfaces of the anodized electrodes[16] are very difficult to treat theoretically, and our model of an inhomogeneous array of hemispheroids is certainly only a rough approximation to the surface morphology. Slight roughness can probably best be treated as a perturbation from a smooth surface, where the approximate translational symmetry makes a momentum-space treatment more tractable. However, the extreme roughness of the electrode surfaces, and localized nature of the excitations implied by the measured values of Ω and its dependence on ω_{ex}, suggests that a real-space treatment, as used here, is more suitable. In this theory, we have considered isolated, individual protrusions, and have neglected plasmon-plasmon interactions because we assume that protrusions of the same aspect ratio are separated by more than λ_{ex}/n. However, the effects of nearby protrusions of different sizes may still have some influence on the plasmon.

To explain the observed dependence of Ω on ω_{ex} and to parametrize the spheroids in a simple manner, we make a further assumption about the protrusions that can scatter effectively. The acoustic-mode frequency Ω depends on the size of the protrusion a, while the plasmon frequency depends on the aspect ratio a/b, because we are working in the dipole limit $a, b \ll \lambda$. In order to obtain a one-to-one correspondence of Ω to ω_{ex}, which is required for comparison to our data, we have made the additional assumption that the most effective scattering is from protrusions of a particular value of b, requiring a peak in $P(b)$. It is also possible, however, that the RS intensity may be maximized from features of this size. This might occur because of the balance between the effects of wall collisions causing additional damping of the plasmon for very small protrusions and retardation limiting the contribution to the RS from larger protrusions. Thus, while the theory is only an approximate treatment of the rough surface, we are able to obtain agreement with the experimental observations, and the theory can offer some insight into the origin of SERS.

For the case of metal sols, however, this treatment is probably quite a good model. We have predicted and observed inelastic Mie scattering from metallic spheroids caused by a mechanical oscillation of the particles themselves. We have experimentally observed this effect when the RS cross section is enhanced by using the resonance of the dipolar surface plasmon to couple light in and out. We have also observed the additional inelastic Rayleigh scattering from surface-adsorbed molecules. The observed RS has the unusual property that the frequency shifts with excitation energy. The inelastic Mie scattering yields information on the distribution of spheroid sizes. We expect that with a judicious choice of excitation energy and spectrometer (i.e., Fabry-Perot or grating spectrometer) this inelastic Mie scattering should be observable from a variety of systems, and may allow the use of relatively simple optical spectroscopies to probe the distribution of sizes and shapes of a collection of spheroids.

[1]H. C. Van de Hulst, *Light Scattering by Small Particles* (Wiley, New York, 1957).
[2]For a recent review see R. P. Van Duyne, *Chemical and Biological Applications of Lasers*, edited by C. B. Moore (Academic, New York, 1978), Vol. 4.
[3]J. I. Gersten and A. Nitzan, J. Chem. Phys. 73, 3023 (1980).
[4]D. Weitz, A. Z. Genack, T. J. Gramila, and J. I. Gersten, Phys. Rev. Lett. 45, 355 (1980).
[5]J. C. Maxwell-Garnett, Philos. Trans. R. Soc. London 203, 385 (1904); 205, 237 (1906).
[6]J. C. Tsang, J. R. Kirtley, and J. A. Bradley, Phys. Rev. Lett. 43, 772 (1979).
[7]T. K. Lee and J. L. Birman (unpublished).

[8]P. B. Johnson and R. W. Christy, Phys. Rev. B 6, 4370 (1972).
[9]R. W. Cohen, G. D. Cody, M. D. Couts, and B. Abeles, Phys. Rev. B 8, 3689 (1973).
[10]A. E. H. Love, *Mathematical Theory of Elasticity*, 3rd ed. (Cambridge University Press, Cambridge, 1920).
[11]D. L. Jeanmaire and R. P. Van Duyne, J. Electroanal. Chem. 84, 1 (1977).
[12]J. A. Creighton, C. G. Blatchford, and M. G. Albrecht, J. Chem. Soc. Faraday Trans. II 75, 790 (1979).
[13]M. Moscovits, J. Chem. Phys. 69, 4159 (1978); Solid State Commun. 32, 59 (1979); E. Burstein, C. Y. Chen, and S. Lundquist, in *Proceedings of the Joint* US-USSR *Symposium on the Theory of Light Scattering in Condensed Matter, New York, 1979*, edited by J. L. Birman, H. Z. Cummins, and K. K. Rebane (Plenum, New York, 1979).
[14]A. Z. Genack, D. A. Weitz, and T. J. Gramila, Surf. Sci. (in press).
[15]H. Morawitz and T. R. Koehler, Chem. Phys. Lett. 71, 64 (1980).
[16]J. F. Evans, M. G. Albrecht, D. M. Ullevig, and R. M. Hexter, J. Electroanal. Chem. 106, 209 (1980).